Interplay of Thermalization and Strong Disorder: Wave Turbulence Theory, Numerical Simulations, and Experiments in Multimode Optical Fibers

Nicolas Berti,[1] Kilian Baudin,[1] Adrien Fusaro,[2] Guy Millot,[1,3] Antonio Picozzi,[1] and Josselin Garnier[4]

[1]*Laboratoire Interdisciplinaire Carnot de Bourgogne, CNRS, Université Bourgogne Franche-Comté, 21000 Dijon, France*
[2]*CEA, DAM, DIF, F-91297 Arpajon Cedex, France*
[3]*Institut Universitaire de France (IUF), 1 Rue Descartes, 75005 Paris, France*
[4]*CMAP, CNRS, Ecole Polytechnique, Institut Polytechnique de Paris, 91128 Palaiseau Cedex, France*

(Received 4 April 2022; accepted 7 July 2022; published 3 August 2022)

We address the problem of thermalization in the presence of a time-dependent disorder in the framework of the nonlinear Schrödinger (or Gross-Pitaevskii) equation with a random potential. The thermalization to the Rayleigh-Jeans distribution is driven by the nonlinearity. On the other hand, the structural disorder is responsible for a relaxation toward the homogeneous equilibrium distribution (particle equipartition), which thus inhibits thermalization (energy equipartition). On the basis of the wave turbulence theory, we derive a kinetic equation that accounts for the presence of strong disorder. The theory unveils the interplay of disorder and nonlinearity. It unexpectedly reveals that a nonequilibrium process of condensation and thermalization can take place in the regime where disorder effects dominate over nonlinear effects. We validate the theory by numerical simulations of the nonlinear Schrödinger equation and the derived kinetic equation, which are found in quantitative agreement without using any adjustable parameter. Experiments realized in multimode optical fibers with an applied external stress evidence the process of thermalization in the presence of strong disorder.

DOI: 10.1103/PhysRevLett.129.063901

Introduction.—A nonintegrable Hamiltonian system of random waves is expected to exhibit a process of thermalization, which is characterized by an irreversible evolution toward the thermodynamic equilibrium state of maximum entropy. In the weakly nonlinear regime, this process is described in detail by the well-developed wave turbulence theory [1–9]. In spite of the formal reversibility of the Hamiltonian system, the wave turbulence kinetic equation describes the actual irreversible evolution to the Rayleigh-Jeans (RJ) equilibrium distribution. RJ thermalization can be characterized by a process of wave condensation that is featured by the macroscopic population of the fundamental mode of the system [2–4,10–18]. This phenomenon received a recent renewed interest with the discovery of spatial beam cleaning in multimode optical fibers (MMFs) [19–21]. Along this line, RJ thermalization and light condensation in MMFs have been discussed [22–28] and recently observed experimentally [29–33].

On the other hand, a structural disorder of the nonlinear medium is known to deeply affect the coherence properties of the waves. Understanding the interplay of nonlinearity and disorder is a fundamental problem, in relation with the paradigm of statistical light-mode dynamics, glassy behaviors, and complexity science [34–42]. Disorder is also known to impact light propagation in MMFs, a feature relevant to endoscopic imaging [43,44], or to study completely integrable Manakov systems [45–48]. Because of refractive index fluctuations introduced by inherent imperfections and environmental perturbations, a MMF leads to both polarization mixing and random mode coupling [45–49]. While polarization random fluctuations, i.e., "weak disorder," have been shown to accelerate the process of beam-cleaning condensation in MMFs [23,25], so far, the interplay of "strong disorder" (i.e., random coupling among nondegenerate modes) and thermalization has not yet been considered.

In this Letter, we address the problem of thermalization of random waves that propagate in a disordered system by considering the representative example of the nonlinear Schrödinger (NLS), or Gross-Pitaevskii, equation with a time-dependent random potential. On the basis of the wave turbulence theory [1–9], we derive a kinetic equation (KE) that accounts for the presence of a time-dependent strong disorder. Our theory describes in detail the antagonist impacts of nonlinearity and disorder. While strong disorder enforces a relaxation to the homogeneous equilibrium distribution of the modal components ("particle" equipartition, $w_j^{\mathrm{eq}} = \mathrm{const}$, w_j being the occupation of the jth mode), the nonlinear process of thermalization favors the macroscopic population of the condensed fundamental mode ($w_0 \gg w_j$ for $j \neq 0$). The remarkable result of our Letter is to show that, despite the dominant strength of disorder, the system can exhibit an unexpected process of "nonequilibrium condensation" in the initial evolution stage, while the system eventually relaxes to the homogeneous equilibrium distribution dictated by strong disorder. The theory is confirmed by intensive numerical simulations of the NLS equation, which are found in quantitative agreement with the simulations of the derived KE, without using any adjustable parameter. We report experiments in MMFs with an applied external stress to control the strength of disorder, which evidences the process of RJ thermalization and condensation in the presence of strong disorder.

Our Letter paves the way for the development of a systematic method to tackle the impact of a time-dependent disorder in wave turbulence—our methodology substantially differs from that developed for a time-independent disorder [38–42]. More generally, this Letter contributes to the understanding of spontaneous organization of coherent states in nonlinear disordered systems [34–38].

NLS equation with random potential.—We consider the general form of the stochastic NLS equation

$$i\partial_z\psi = -\alpha\nabla^2\psi + V(\boldsymbol{r})\psi - \gamma|\psi|^2\psi + \delta V(\boldsymbol{r},z)\psi. \quad (1)$$

It governs the transverse spatial evolution of an optical beam propagating along the z axis of a waveguide, whose ideal transverse index profile is $V(\boldsymbol{r})$ [$\boldsymbol{r}=(x,y)$], while $\delta V(\boldsymbol{r},z)$ is the "time"-dependent random perturbation of the potential ($\langle\delta V\rangle = 0$). The parameters α and γ denote the linear and nonlinear coefficients. The disorder being ("time") z dependent, our system is of different nature than those studying the interplay of thermalization and Anderson localization [38–42].

We expand the field $\psi(\boldsymbol{r},z)=\sum_j a_j(z)u_j(\boldsymbol{r})$ on the basis of the M real-valued eigenmodes $u_j(\boldsymbol{r})$ (solution of $\beta_j u_j = -\alpha\nabla^2 u_j + V(\boldsymbol{r})u_j$) of the unperturbed waveguide. The mode amplitudes $a_j(z)$ satisfy

$$i\partial_z a_j = \beta_j a_j - \gamma\sum_{l,m,n} Q_{jlmn} a_l a_m a_n^* + \sum_l C_{jl}(z)a_l, \quad (2)$$

where $Q_{jlmn} = \int u_j(\boldsymbol{r})u_l(\boldsymbol{r})u_m(\boldsymbol{r})u_n(\boldsymbol{r})d\boldsymbol{r}$ denotes the mode overlap, and the random mode coupling matrix reads

$$C_{jl}(z) = \int u_j(\boldsymbol{r})\delta V(z,\boldsymbol{r})u_l(\boldsymbol{r})d\boldsymbol{r}. \quad (3)$$

The stochastic NLS [Eq. (1)] and the modal NLS [Eq. (2)] are equivalent. They conserve the total power (particle number) $N = \int|\psi|^2 d\boldsymbol{r} = \sum_j |a_j|^2$, while the random potential $\delta V(\boldsymbol{r},z)$ in Eq. (1) [or $\boldsymbol{C}(z)$ in Eq. (2)], prevents the conservation of the energy (Hamiltonian).

Kinetic equation.—We consider the situation where the random potential is a weak perturbation with respect to linear propagation effects ($\delta V \ll V$), i.e., $L_{\rm lin} = 1/\beta_0 \ll L_{\rm dis} = 1/\sigma$ and $L_{\rm lin} \ll \ell_c$, where σ^2 denotes the variance of the fluctuations of the random potential (i.e., "strength" of disorder) and ℓ_c the corresponding correlation length. Note that this is the usual case in an optical waveguide configuration, e.g., in MMFs. Furthermore, we assume that disorder dominates over nonlinear effects $L_{\rm dis} \ll L_{\rm nl} \simeq 1/(\gamma\langle|\psi|^2\rangle)$.

We develop a wave turbulence theory [1–9] accounting for a time-dependent disorder by exploiting tools inherited from the asymptotic analysis of randomly driven ordinary differential equations [50]. We derive the KE governing the evolution of the averaged modal components $w_j(z) = \langle|a_j(z)|^2\rangle$ [51]:

$$\partial_z w_j = \sum_{l\neq j}\Gamma^{\rm OD}_{jl}(w_l - w_j) + \mathcal{C}oll_j[\boldsymbol{w}] \quad (4)$$

where the collision term reads

$$\mathcal{C}oll_j[\boldsymbol{w}] = 8\gamma^2\sum_{l,m,n}\frac{\delta^K_{jlmn}Q^2_{jlmn}}{G^D_{jlmn}}R_{jlmn}[\boldsymbol{w}],$$
$$R_{jlmn}[\boldsymbol{w}] = w_l w_m w_j + w_l w_m w_n - w_j w_n w_m - w_j w_n w_l,$$

and the Kronecker symbol denotes a frequency resonance ($\delta^K_{jlmn} = 1$ if $\Delta\beta_{jlmn} = \beta_j - \beta_l - \beta_m + \beta_n = 0$, and zero otherwise). For clarity, we assume that the modes are not degenerate—see [51] for the KE accounting for mode degeneracies.

The KE [Eq. (4)] unveils the interplay of nonlinearity and disorder. It reveals that diagonal and off-diagonal elements of the random matrix $\boldsymbol{C}$ play fundamental different roles. The first term in the KE [Eq. (4)] originates in *off-diagonal* elements of C_{jl} ($j \neq l$):

$$\Gamma^{\rm OD}_{jl} = 2\int_0^\infty\langle C_{jl}(0)C_{jl}(z)\rangle\cos[(\beta_j - \beta_l)z]dz. \quad (5)$$

It describes an irreversible relaxation toward the homogeneous distribution featured by an equipartition of "particles" among the modes, $w^{\rm eq}_j = N/M = \text{const}$. This process occurs over the typical propagation length [54]

$$\mathcal{L}^{\rm eq}_{\rm kin} \simeq 1/\overline{\Gamma^{\rm OD}_{jl}}. \quad (6)$$

This is the well-known evolution of a system ruled by random mode coupling.

We now show that this relaxation process mediated by strong disorder does not necessarily inhibit the nonlinear processes of thermalization and condensation. This becomes apparent through the collision term in the KE [Eq. (4)], which exclusively involves the *diagonal* components C_{jj}:

$$\Gamma^D_{jl} = \int_0^\infty\langle C_{jj}(0)C_{ll}(z)\rangle + \langle C_{ll}(0)C_{jj}(z)\rangle dz. \quad (7)$$

The matrix $\boldsymbol{\Gamma}^D$ contributes to the tensor involved in the collision term, $G^D_{jlmn} = \Gamma^D_{ll} + \Gamma^D_{mm} + \Gamma^D_{nn} + \Gamma^D_{jj} + 2\Gamma^D_{lm} - 2\Gamma^D_{ln} - 2\Gamma^D_{lj} - 2\Gamma^D_{mn} - 2\Gamma^D_{mj} + 2\Gamma^D_{nj}$ [51]. To discuss the role of the collision term, we forget for a while the first term in the KE [Eq. (4)]. The collision term conserves $N = \sum_j w_j(z)$, $E = \sum_j \beta_j w_j(z)$, and exhibits a H theorem of entropy growth $\partial_z S \geq 0$, with $S(z) = \sum_j \log[w_j(z)]$ [51]. Hence, it describes a process of thermalization to the RJ distribution $w_j^{\mathrm{RJ}} = T/(\beta_j - \mu)$, which occurs over a typical propagation length,

$$\mathcal{L}_{\mathrm{kin}}^{\mathrm{RJ}} \simeq L_{\mathrm{nl}}^2 \overline{G_{jlmn}^{\mathrm{D}}/Q_{jlmn}^2}. \tag{8}$$

For an energy smaller than a critical value $E \leq E_{\mathrm{crit}} \simeq N\beta_0\sqrt{M/2}$, the RJ distribution w_j^{RJ} exhibits a phase transition to a condensed state [29]. The condensate amplitude w_0 then constitutes the natural parameter that distinguishes the two antagonist regimes: (i) For $\mathcal{L}_{\mathrm{kin}}^{\mathrm{eq}} \ll \mathcal{L}_{\mathrm{kin}}^{\mathrm{RJ}}$, the disorder dominates and $w_0(z) \to w_j^{\mathrm{eq}} = N/M = \mathrm{const}$ for $j = 0, 1, \ldots, M-1$; (ii) For $\mathcal{L}_{\mathrm{kin}}^{\mathrm{eq}} \gg \mathcal{L}_{\mathrm{kin}}^{\mathrm{RJ}}$, the dynamics is dominated by RJ thermalization, and condensation leads to a macroscopic population of the fundamental mode $w_0(z) \to w_0^{\mathrm{RJ}} \gg w_j^{\mathrm{RJ}}$ for $j = 1, \ldots, M-1$.

Numerical simulations.—We have performed numerical simulations to test the validity of our theory. We have considered the concrete example of a parabolic trapping potential of the form $V(\boldsymbol{r}) = q_x x^2 + q_y y^2$, with the fundamental mode eigenvalue $\beta_0 = \sqrt{\alpha}(\sqrt{q_x} + \sqrt{q_y})$. We consider a general model of disorder with a random potential of the form $\delta V(\boldsymbol{r}, z) = \mu(z) g(\boldsymbol{r})$, where $\mu(z)$ is a real-valued stochastic function with zero mean and $\langle \mu(0)\mu(z)\rangle = \sigma^2 \exp(-|z|/\ell_c)$. In order to remove mode degeneracies, we consider in the simulations an elliptical parabolic potential ($q_x \neq q_y$). To compute the matrices $\boldsymbol{\Gamma}^{\mathrm{OD}}$ and $\boldsymbol{\Gamma}^{D}$ in analytical form we consider $g(x, y) = \cos(b_x x/x_0) \times \cos(b_y y/y_0)$, where (x_0, y_0) denote the radii of the fundamental elliptical mode [51].

According to the theory, the two terms in the KE [Eq. (4)] are antagonists and compete against each other. If $\mathcal{L}_{\mathrm{kin}}^{\mathrm{eq}} \ll \mathcal{L}_{\mathrm{kin}}^{\mathrm{RJ}}$, disorder prevails and the system relaxes to the expected equilibrium $w_j^{\mathrm{eq}} = \mathrm{const}$. This is illustrated in Fig. 1, which reports the results of the numerical integration of the NLS Eq. (2) for 64 realizations ($\mathcal{L}_{\mathrm{kin}}^{\mathrm{RJ}}/\mathcal{L}_{\mathrm{kin}}^{\mathrm{eq}} \simeq 400$). The corresponding average over such realizations (bold white line) is in agreement with the simulation of the KE [Eq. (4)] (dashed black line) starting from the same initial condition. Here and thereafter, the quantitative agreement between NLS and KE simulations is obtained without any adjustable parameter.

Unexpectedly, however, a "nonequilibrium" process of condensation and thermalization can be observed in the initial stage of propagation when $\mathcal{L}_{\mathrm{kin}}^{\mathrm{RJ}} \lesssim \mathcal{L}_{\mathrm{kin}}^{\mathrm{eq}}$ (see Fig. 2 for $\mathcal{L}_{\mathrm{kin}}^{\mathrm{RJ}}/\mathcal{L}_{\mathrm{kin}}^{\mathrm{eq}} \simeq 0.07$), while asymptotically the system still relaxes to the homogeneous equilibrium state w_j^{eq}. The nonequilibrium property of condensation is reflected by the

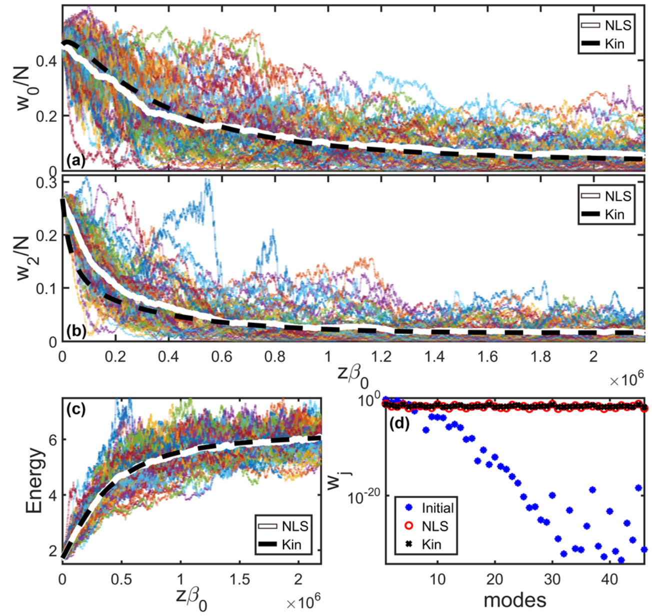

FIG. 1. Dynamics dominated by strong disorder $\mathcal{L}_{\mathrm{kin}}^{\mathrm{RJ}} \gg \mathcal{L}_{\mathrm{kin}}^{\mathrm{eq}}$. The system irreversibly relaxes toward the equilibrium w_j^{eq}. Evolutions of the fundamental mode $w_0(z)$ (a), and $w_2(z)$ (b), the energy $E(z)/(N\beta_0)$ (c), obtained from the numerical simulation of the NLS Eq. (2). Sixty-four realizations are reported with colored lines; the bold white line is the corresponding empirical average; the dashed black line is the prediction of the KE [Eq. (4)]. (d) Modal distribution w_j in the initial condition ($z = 0$, blue) and at $z\beta_0 = 2 \times 10^6$ for the NLS simulation (red), and the KE (black). Parameters: $L_{\mathrm{dis}}/L_{\mathrm{lin}} = 7$, $L_{\mathrm{dis}}/L_{\mathrm{nl}} = 4.1 \times 10^{-4}$, $\ell_c \beta_0 = 42$.

fact that the energy $E(z) = \sum_j \beta_j w_j(z)$ is not conserved during the evolution; see Fig. 2(c).

We stress that the condensation processes can occur very efficiently by increasing the correlation length ℓ_c, in such a way that $\mathcal{L}_{\mathrm{kin}}^{\mathrm{RJ}} \ll \mathcal{L}_{\mathrm{kin}}^{\mathrm{eq}}$; see Fig. 3 for $\mathcal{L}_{\mathrm{kin}}^{\mathrm{RJ}}/\mathcal{L}_{\mathrm{kin}}^{\mathrm{eq}} \simeq 0.003$. In this regime, the energy is almost conserved $E \simeq \mathrm{const}$ and RJ thermalization occurs almost completely, as confirmed by the modal populations that approach the RJ distribution w_j^{RJ} [Fig. 3(d)], and the condensate approaches the RJ prediction $w_0^{\mathrm{RJ}}/N \simeq 0.55$; see Fig. 3(a). Note that, for $z \gg \mathcal{L}_{\mathrm{kin}}^{\mathrm{eq}}$, the system would still relax to the equilibrium w_j^{eq}.

Experiments.—We performed experiments in a MMF to evidence light condensation in the presence of strong disorder. The subnanosecond pulses delivered by a Nd:YAG laser ($\lambda = 1.06$ μm) are passed through a diffuser before injection into a 12 m long graded-index MMF [i.e., parabolic-shaped potential $V(\boldsymbol{r})$] that guides $M \simeq 120$ modes. We measure the power N and the energy E from the near-field and far-field measurements of the intensity distributions at the fiber output; see Ref. [29] for details.

Here, the originality with respect to all previous experiments on beam-cleaning condensation and thermalization

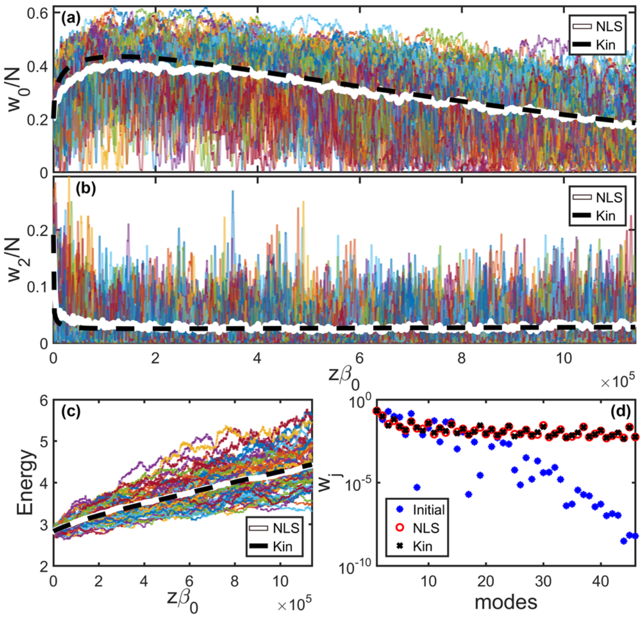

FIG. 2. Thermalization precedes equilibrium relaxation. Same panels as in Fig. 1, but in the regime $\mathcal{L}_{\rm kin}^{\rm RJ} \lesssim \mathcal{L}_{\rm kin}^{\rm eq}$. The system exhibits an incipient process of RJ thermalization and nonequilibrium condensation characterized by a growth of the condensate amplitude $w_0(z)$ for $z\beta_0 \lesssim 2\times 10^5$. Disorder subsequently prevails, which induces a decay of $w_0(z)$ (and eventually brings the system to equilibrium $w_j^{\rm eq}$). Parameters: $L_{\rm dis}/L_{\rm lin} = 7$, $L_{\rm dis}/L_{\rm nl} = 0.033$, and $\ell_c\beta_0 = 167$.

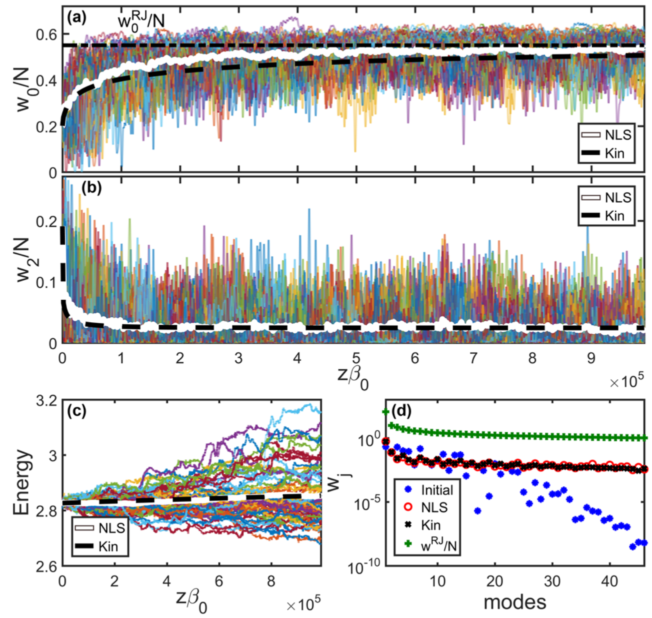

FIG. 3. Thermalization prevails over equilibrium relaxation. Same panels as in Fig. 1, but in the regime $\mathcal{L}_{\rm kin}^{\rm RJ} \ll \mathcal{L}_{\rm kin}^{\rm eq}$. The system exhibits a process of RJ thermalization and condensation characterized by a significant growth of the condensate amplitude $w_0(z)$ to the value predicted by the RJ distribution, $w_0^{\rm RJ}/N \simeq 0.55$ (horizontal dashed-dotted black line) (a). At variance with Figs. 1 and 2, the energy $E(z)$ is almost constant (c). The modes approach the RJ distribution $w_j^{\rm RJ}$ (green) (d). Parameters: $L_{\rm dis}/L_{\rm lin} = 8.4$, $L_{\rm dis}/L_{\rm nl} = 0.04$, and $\ell_c\beta_0 = 4\times 10^3$.

[19–21,29–32] is that we introduce strong disorder in the experiment. Strong mode coupling is obtained by applying a stress to the MMF with clamps [49]. By adjusting the applied stress, we can tune the strength of mode coupling (i.e., σ). In the absence of an applied stress, polarization coupling and random coupling among degenerate modes take place: In this weak random coupling regime, the energy $E = \sum_j \beta_j w_j$ is conserved during light propagation in the MMF [23,25], as confirmed by direct experimental measurements [24,29–32]. Here, we apply stress on the MMF to induce a random coupling among nondegenerate modes [45–48,55]. In this regime of strong mode coupling, the energy E is no longer conserved through propagation in the MMF. Note that, it would be difficult, or even impossible, to accurately model in the simulations the peculiar form of disorder induced by the applied stress on the fiber. Furthermore, the simulations reported above do not account for the mode degeneracies of the fiber used in the experiments. Accordingly, the simulations do not describe quantitatively our experiments.

We report in Fig. 4(a) the measurements of the condensate fraction w_0/N at small power (linear regime), strong power (nonlinear regime), and in the presence, or absence, of applied stress. Following Ref. [29], the diffuser allows us to vary the energy density E/N of the injected speckle beam. The squares in Fig. 4(a) report the corresponding condensate fractions w_0/N in the linear and nonlinear regimes in the absence of strong disorder. For each speckle beam with energy E/N [i.e., for each color in Fig. 4(a)], we apply stress on different points of the fiber to get an ensemble of 10 realizations with disorder. We report in Fig. 4(a) the corresponding values of w_0/N for such 10 realizations (small circles), as well as the corresponding average over realizations (large circles). Because the applied stress on the MMF induces power losses [10% in Fig. 4(a)] [49], we normalize the energy with respect to the (average) power: $E/N = \sum_j \beta_j w_j / \sum_j w_j = \overline{\beta_j}$. Strong random mode coupling leads to an *increase* of E/N, as evidenced in Fig. 4(a), where the squares are shifted to the big circles by an amount of $\Delta\overline{E/N} \simeq 6\%$. The larger the strength of applied stress, the larger the energy shift $\Delta\overline{E/N}$.

Figure 4(a) remarkably reveals that, by increasing the power from the linear regime ($N = 0.23$ kW) to the nonlinear regime ($N = 7$ kW), the condensate fraction w_0/N (big circles) increases and approaches the value predicted by the RJ distribution $w_0^{\rm RJ}/N$ (solid line). Thermalization then takes place: (i) in the presence of strong disorder, i.e., in the presence of an energy shift $\Delta\overline{E/N}$; (ii) over a broad range of E/N, i.e., broad range of condensate fractions. Note that, the presence of losses, distributed either

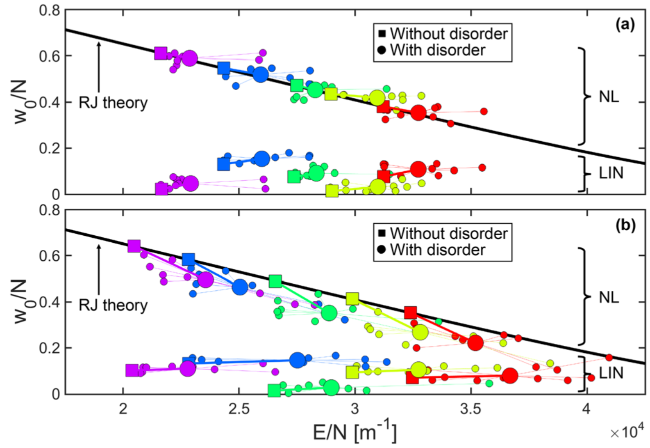

FIG. 4. Observation of light condensation with strong disorder. Measurements of the condensate fraction w_0/N vs E/N at small power [linear (LIN) regime] and high power [nonlinear (NL) regime], for a moderate (a), and a large (b), strength of random mode coupling. The solid line reports the prediction from the RJ theory, w_0^{RJ}/N. In the absence of strong disorder (squares), w_0/N increases as the power increases, and reaches the RJ prediction (solid line)—each color refers to a different value of E/N. In the presence of strong disorder (big circles), the energy E/N increases due to disorder (squares are shifted to big circles of the same color), by $\Delta\overline{E/N} \simeq 6\%$ (a), and $\Delta\overline{E/N} \simeq 11\%$ (b). The big circles report the average over 10 different realizations of disorder (10 small circles for each color). RJ thermalization takes place in the presence of strong disorder (a), and it is quenched by further increasing the amount of disorder (b) [51].

homogeneously or nonhomogeneously among the modes, does not significantly affect the condensate fraction [51].

We have repeated the procedure of Fig. 4(a) by increasing the applied stress on the MMF with an energy shift $\Delta\overline{E/N} \simeq 11\%$ (20% of power losses). As evidenced in Fig. 4(b), $\Delta\overline{E/N}$ is larger than in Fig. 4(a). Consequently, the condensate fractions w_0/N in the nonlinear regime no longer reach the RJ prediction, i.e., strong disorder prevents a complete process of RJ thermalization and condensation. By further increasing the applied stress and the corresponding energy shift $\Delta\overline{E/N} \simeq 19\%$, our experimental results show that RJ thermalization is inhibited by strong disorder; see Ref. [51].

Conclusion.—We have developed a wave turbulence theory that accounts for a "time"-dependent disorder by considering the NLS equation with a random potential. Simulations of the derived KE [Eq. (4)] are found in quantitative agreement with NLS simulations without using any adjustable parameter. The theory remarkably reveals that RJ thermalization and condensation can take place efficiently in the presence of strong disorder, as confirmed by experiments realized in MMFs.

The developed wave turbulence theory can be extended to dissipative systems [56,57], or to different types of disordered nonlinear systems, e.g., Bose-Einstein condensates, hydrodynamics, condensed matter, etc.

The authors are grateful to K. Krupa and S. Rica for fruitful discussions. This work was supported by the Centre national de la recherche scientifique (CNRS), Conseil régional de Bourgogne Franche-Comté, iXCore Research Foundation, Agence Nationale de la Recherche (ANR-19-CE46-0007, ANR-17-EURE-0002, ANR-15-IDEX-0003, ANR-21-ESRE-0040). Calculations were performed using HPC resources from DNUM CCUB (Centre de Calcul, Université de Bourgogne).

[1] V. E. Zakharov, V. S. L'vov, and G. Falkovich, *Kolmogorov Spectra of Turbulence I* (Springer, Berlin, 1992).

[2] A. C. Newell, S. Nazarenko, and L. Biven, Wave turbulence and intermittency, Physica (Amsterdam) **152D**, 520 (2001).

[3] S. Nazarenko, *Wave Turbulence*, Lectures Notes in Physics (Springer, New York, 2011).

[4] A. C. Newell and B. Rumpf, Wave turbulence, Annu. Rev. Fluid Mech. **43**, 59 (2011).

[5] *Advances in Wave Turbulence*, World Scientific Series on Nonlinear Science Series A Vol. 83, edited by V. I. Shrira (World Scientific, Singapore, 2013).

[6] J. Laurie, U. Bortolozzo, S. Nazarenko, and S. Residori, One-dimensional optical wave turbulence: Experiment and theory, Phys. Rep. **514**, 121 (2012).

[7] V. S. L'vov and S. V. Nazarenko, Discrete and mesoscopic regimes of finite-size wave turbulence, Phys. Rev. E **82**, 056322 (2010).

[8] M. Onorato, L. Vozella, D. Proment, and Y. V. L'vov, Route to thermalization in the α−Fermi-Pasta-Ulam system, Proc. Natl. Acad. Sci. U.S.A. **112**, 4208 (2015).

[9] A. Picozzi, J. Garnier, T. Hansson, P. Suret, S. Randoux, G. Millot, and D. N. Christodoulides, Optical wave turbulence: Toward a unified nonequilibrium thermodynamic formulation of statistical nonlinear optics, Phys. Rep. **542**, 1 (2014).

[10] C. Connaughton, C. Josserand, A. Picozzi, Y. Pomeau, and S. Rica, Condensation of Classical Nonlinear Waves, Phys. Rev. Lett. **95**, 263901 (2005).

[11] N. G. Berloff and A. J. Youd, Dissipative Dynamics of Superfluid Vortices at Nonzero Temperatures, Phys. Rev. Lett. **99**, 145301 (2007).

[12] G. Düring, A. Picozzi, and S. Rica, Breakdown of weak-turbulence and nonlinear wave condensation, Physica (Amsterdam) **238D**, 1524 (2009).

[13] G. Krstulovic and M. Brachet, Energy cascade with small-scale thermalization, counterflow metastability, and anomalous velocity of vortex rings in Fourier-truncated Gross-Pitaevskii equation, Phys. Rev. E **83**, 066311 (2011).

[14] S. Nazarenko, M. Onorato, and D. Proment, Bose-Einstein condensation and Berezinskii-Kosterlitz-Thouless transition in the two-dimensional nonlinear Schrödinger model, Phys. Rev. A **90**, 013624 (2014).

[15] A. Rückriegel and P. Kopietz, Rayleigh-Jeans Condensation of Pumped Magnons in Thin-Film Ferromagnets, Phys. Rev. Lett. **115**, 157203 (2015).

[16] A. Chiocchetta, P. E. Larré, and I. Carusotto, Thermalization and Bose-Einstein condensation of quantum light in bulk nonlinear media, Europhys. Lett. **115**, 24002 (2016).

[17] N. Santic, A. Fusaro, S. Salem, J. Garnier, A. Picozzi, and R. Kaiser, Nonequilibrium Precondensation of Classical Waves in Two Dimensions Propagating through Atomic Vapors, Phys. Rev. Lett. **120**, 055301 (2018).

[18] J. Bloch, I. Carusotto, and M. Wouters, Spontaneous coherence in spatially extended photonic systems: Non-equilibrium Bose-Einstein condensation, Nat. Phys. Rev. **4**, 470 (2022).

[19] K. Krupa, A. Tonello, A. Barthélémy, V. Couderc, B. M. Shalaby, A. Bendahmane, G. Millot, and S. Wabnitz, Observation of Geometric Parametric Instability Induced by the Periodic Spatial Self-Imaging of Multimode Waves, Phys. Rev. Lett. **116**, 183901 (2016).

[20] L. G. Wright, Z. Liu, D. A. Nolan, M.-J. Li, D. N. Christodoulides, and F. W. Wise, Self-organized instability in graded-index multimode fibres, Nat. Photonics **10**, 771 (2016).

[21] K. Krupa, A. Tonello, B. M. Shalaby, M. Fabert, A. Barthélémy, G. Millot, S. Wabnitz, and V. Couderc, Spatial beam self-cleaning in multimode fibres, Nat. Photonics **11**, 237 (2017).

[22] P. Aschieri, J. Garnier, C. Michel, V. Doya, and A. Picozzi, Condensation and thermalization of classsical optical waves in a waveguide, Phys. Rev. A **83**, 033838 (2011).

[23] A. Fusaro, J. Garnier, K. Krupa, G. Millot, and A. Picozzi, Dramatic Acceleration of Wave Condensation Mediated by Disorder in Multimode Fibers, Phys. Rev. Lett. **122**, 123902 (2019).

[24] E. Podivilov, D. Kharenko, V. Gonta, K. Krupa, O. S. Sidelnikov, S. Turitsyn, M. P. Fedoruk, S. A. Babin, and S. Wabnitz, Hydrodynamic 2D Turbulence and Spatial Beam Condensation in Multimode Optical Fibers, Phys. Rev. Lett. **122**, 103902 (2019).

[25] J. Garnier, A. Fusaro, K. Baudin, C. Michel, K. Krupa, G. Millot, and A. Picozzi, Wave condensation with weak disorder versus beam self-cleaning in multimode fibers, Phys. Rev. A **100**, 053835 (2019).

[26] F. O. Wu, A. U. Hassan, and D. N. Christodoulides, Thermodynamic theory of highly multimoded nonlinear optical systems, Nat. Photonics **13**, 776 (2019).

[27] A. Ramos, L. Fernández-Alcázar, T. Kottos, and B. Shapiro, Optical Phase Transitions in Photonic Networks: A Spin-System Formulation, Phys. Rev. X **10**, 031024 (2020).

[28] F. O. Wu, Q. Zhong, H. Ren, P. S. Jung, K. G. Makris, and D. N. Christodoulides, Thermalization of Light's Orbital Angular Momentum in Nonlinear Multimode Waveguide Systems, Phys. Rev. Lett. **128**, 123901 (2022).

[29] K. Baudin, A. Fusaro, K. Krupa, J. Garnier, S. Rica, G. Millot, and A. Picozzi, Classical Rayleigh-Jeans Condensation of Light Waves: Observation and Thermodynamic Characterization, Phys. Rev. Lett. **125**, 244101 (2020).

[30] H. Pourbeyram, P. Sidorenko, F. Wu, L. Wright, D. Christodoulides, and F. Wise, Direct measurement of thermalization to Rayleigh-Jeans distribution in optical beam self cleaning, Nat. Phys. **18**, 685 (2022).

[31] K. Baudin, A. Fusaro, J. Garnier, N. Berti, K. Krupa, I. Carusotto, S. Rica, G. Millot, and A. Picozzi, Energy and wave-action flows underlying Rayleigh-Jeans thermalization of optical waves propagating in a multimode fiber, Europhys. Lett. **134**, 14001 (2021).

[32] F. Mangini, M. Gervaziev, M. Ferraro, D. S. Kharenko, M. Zitelli, Y. Sun, V. Couderc, E. V. Podivilov, S. A. Babin, and S. Wabnitz, Statistical mechanics of beam self-cleaning in GRIN multimode optical fibers, Opt. Express **30**, 10850 (2022).

[33] E. V. Podivilov, F. Mangini, O. S. Sidelnikov, M. Ferraro, M. Gervaziev, D. S. Kharenko, M. Zitelli, M. P. Fedoruk, S. A. Babin, and S. Wabnitz, Thermalization of Orbital Angular Momentum Beams in Multimode Optical Fibers, Phys. Rev. Lett. **128**, 243901 (2022).

[34] C. Conti and E. DelRe, Photonics and the nobel prize in physics, Nat. Photonics **16**, 6 (2022).

[35] D. Pierangeli, A. Tavani, F. Di Mei, A. J. Agranat, C. Conti, and E. DelRe, Observation of replica symmetry breaking in disordered nonlinear wave propagation, Nat. Commun. **8**, 1501 (2017).

[36] D. Churkin, I. Kolokolov, E. Podivilov, I. Vatnik, S. Vergeles, I. Terekhov, V. Lebedev, G. Falkovich, M. Nikulin, S. Babin, and S. Turitsyn, Wave kinetics of a random fibre laser, Nat. Commun. **2**, 6214 (2015).

[37] M. Segev, Y. Silberberg, and D. N. Christodoulides, Anderson localization of light, Nat. Photonics **7**, 197 (2013).

[38] N. Cherroret, T. Karpiuk, B. Grémaud, and C. Miniatura, Thermalization of matter waves in speckle potentials, Phys. Rev. A **92**, 063614 (2015).

[39] S. Nazarenko, A. Soffer, and M.-B. Tran, On the wave turbulence theory for the nonlinear Schrödinger equation with random potentials, Entropy **21**, 823 (2019).

[40] Z. Wang, W. Fu, Y. Zhang, and H. Zhao, Wave-Turbulence Origin of the Instability of Anderson Localization Against Many-Body Interactions, Phys. Rev. Lett. **124**, 186401 (2020).

[41] T. Scoquart, P.-E. Larré, D. Delande, and N. Cherroret, Weakly interacting disordered Bose gases out of equilibrium: From multiple scattering to superfluidity, Europhys. Lett. **132**, 66001 (2020).

[42] N. Cherroret, T. Scoquart, and D. Delande, Coherent multiple scattering of out-of-equilibrium interacting Bose gases, Ann. Phys. (Amsterdam) **435**, 168543 (2021).

[43] D. Psaltis and C. Moser, Imaging with multimode fibers, Opt. Photonics News **27**, 24 (2016).

[44] P. Caramazza, O. Moran, R. Murray-Smith, and D. Faccio, Transmission of natural scene images through a multimode fibre, Nat. Commun. **10**, 2029 (2019).

[45] A. Mecozzi, C. Antonelli, and M. Shtaif, Nonlinear propagation in multimode fibers in the strong coupling regime, Opt. Express **20**, 11673 (2012).

[46] A. Mecozzi, C. Antonelli, and M. Shtaif, Coupled Manakov equations in multimode fibers with strongly coupled groups of modes, Opt. Express **20**, 23436 (2012).

[47] S. Mumtaz, R. J. Essiambre, and G. P. Agrawal, Nonlinear propagation in multimode and multicore fibers: Generalization of the Manakov equations, J. Lightwave Technol. **31**, 398 (2013).

[48] Y. Xiao, R.-J. Essiambre, M. Desgroseilliers, A. M. Tulino, R. Ryf, S. Mumtaz, and G. P. Agrawal, Theory of intermodal four-wave mixing with random linear mode coupling in few-mode fibers, Opt. Express **22**, 32039 (2014).

[49] W. Xiong, P. Ambichl, Y. Bromberg, B. Redding, S. Rotter, and H. Cao, Spatiotemporal Control of Light Transmission through a Multimode Fiber with Strong Mode Coupling, Phys. Rev. Lett. **117**, 053901 (2016).

[50] J.-P. Fouque, J. Garnier, G. Papanicolaou, and K. Sølna, *Wave Propagation and Time Reversal in Randomly Layered Media* (Springer, New York, 2007).

[51] See Supplemental Material at http://link.aps.org/supplemental/10.1103/PhysRevLett.129.063901 for the theoretical derivation of the KE [Eq. (4)], for the analytical expressions of the matrices $\mathbf{\Gamma}^D$ and $\mathbf{\Gamma}^{\mathrm{OD}}$ used in the simulations, and a complementary description of the experimental methods, which includes Refs. [1,29,50,52,53].

[52] I. S. Gradstein and I. M. Ryzhik, *Tables of Integrals, Sums, Series, and Products* (Academic Press, New York, 1980).

[53] J. R. Fienup, Phase retrieval algorithms: a comparison, Appl. Opt. **21**, 2758 (1982).

[54] More exactly, $\mathcal{L}_{\mathrm{kin}}^{\mathrm{eq}} = 1/\lambda_2^{\mathrm{OD}}$, where $-\lambda_2^{\mathrm{OD}}$ is the second eigenvalue of the matrix $\tilde{\mathbf{\Gamma}}^{\mathrm{OD}}$, with $\tilde{\Gamma}_{jl}^{\mathrm{OD}} = \Gamma_{jl}^{\mathrm{OD}}$ for $j \neq l$ and $\tilde{\Gamma}_{jj}^{\mathrm{OD}} = -\sum_{l\neq j} \Gamma_{jl}^{\mathrm{OD}}$, the first eigenvalue being $\lambda_1^{\mathrm{OD}} = 0$.

[55] K.-P. Ho and J. M. Kahn, Linear propagation effects in mode-division multiplexing systems, J. Lightwave Technol. **32**, 4 (2014).

[56] R. Weill, B. Fischer, and O. Gat, Light-Mode Condensation in Actively-Mode-Locked Lasers, Phys. Rev. Lett. **104**, 173901 (2010).

[57] E. Turitsyna, S. Smirnov, S. Sugavanam, N. Tarasov, X. Shu, S. Babin, E. Podivilov, D. Churkin, G. Falkovich, and S. Turitsyn, The laminar-turbulent transition in a fibre laser, Nat. Photonics **7**, 783 (2013).